

# The Stoner-Wohlfarth model of Ferromagnetism: Dynamic and Statistical properties

C. Tannous and J. Gieraltowski

*Laboratoire de Magnétisme de Bretagne - CNRS FRE 2697*

*Université de Bretagne Occidentale -*

*6, Avenue le Gorgeu C.S.93837 - 29238 Brest Cedex 3 - FRANCE*

The physics of magnetic state change in single domain magnetic grains (called Stoner particles) is interesting from the fundamental as well as the applied points of view. A change in magnetization can be finely tuned with a specific time variation of an externally applied magnetic field. It may also occur naturally (without application of a field) at very low temperature with quantum tunneling and at higher temperature with thermal excitation. The optimal (usually shortest) time altering the magnetisation along with the smallest applied magnetic field are sought in technological applications such as high-density reading or writing of information, spintronics, quantum information and quantum communication systems.

This work reviews the magnetization change with a time dependent field and temperature and discusses the time it takes to alter the magnetization as a function of the control parameter chosen, temperature and material parameters.

PACS numbers: 51.60.+a, 74.25.Ha, 75.00.00, 75.60.Ej, 75.60.Jk, 75.75.+a

Keywords: Magnetic properties. Magnetic materials. Hysteresis. Magnetization reversal mechanisms. Magnetic properties of nanostructures

## I. INTRODUCTION

The effect of time dependent fields on magnetization state is important for the reading and writing of information and the monitoring of the magnetization in a magnetic material. In the case of magnetic recording, when density is increased, the grain size making the recording media decreases. If it is small enough, its magnetization becomes extremely sensitive to thermal energy; it can flip (in the vertical case) or reverse (in the horizontal case) by the simple effect of (even small) finite temperature perturbation (Brownian fluctuations). This adverse effect is called super-paramagnetism that traditionally limits longitudinal recording of hard disks to densities on the order of 100 Gbits/in<sup>2</sup>. Longitudinal refers to the fact the rotation velocity of the disk is parallel to the magnetization orientation. In perpendicular recording this limit is ten times higher around several Tbits/in<sup>2</sup>.

Progress in size reduction toward the nanometer paves the way to new opportunities in the emerging field of spintronics [1]. On that scale, we have a wide panel of physical effects (e.g. new types of quantum exchange between nanometer thick magnetic layers) and the spin diffusion length becomes long enough to maintain useful spin orientation. Novel nanometric magnetic devices are good candidates for use as building blocks of spintronics (spin diode or spin transistor) or quantum information systems. The latter span quantum information storage (Q-bits), quantum computing (quantum logic operations like the square root of the *NOT* operation ( $\sqrt{NOT}$ ) or the controlled *NOT* operation (*CNOT*), the Quantum Fast Fourier Transform...), quantum communication systems (an example is entanglement which means that measurement performed on one system seems to be

instantaneously influencing other systems related to it) or Quantum Metrology.

It is important to be able to tell how one might be able to alter some state with a magnetic field, or how it might be affected by temperature as in the recording case. It is important to point out that interesting quantum phenomena might occur at low temperatures ( $T \sim 0K$ ) such as magnetic quantum tunneling; while this is beyond the scope of this paper, the reader might consult a review such as ref. [2].

The time it takes for an effect to take place is also important. In recording, given a fixed rotational velocity of the hard disk (typically 7200 rpm) the decrease of bit length, imposes a faster (higher frequency) process of reading (sensing the magnetization orientation)/writing (changing the magnetization orientation) of the bit. While the shortest time altering the magnetization is required in reading/writing applications, the longest time is required in (long-term) storage with protection of the data against large magnetic fields that might corrupt or even erase the stored information.

In this paper corresponding to the second part of the series on the Stoner-Wohlfarth model, we examine the effects of time dependent field and finite temperature on a single domain Stoner particle [3]. The time it takes for the magnetization to change is also studied with temperature and material parameters.

This paper is organized as follows: in section 2 we examine the evolution of magnetization state with a time dependent field. In section 3 we discuss the effect of temperature on magnetization reversal and we conclude in section 4 with the possible extensions and perspectives

of the SW model.

## II. EQUATION OF MOTION FOR THE MAGNETIZATION IN THE PRESENCE OF A TIME DEPENDENT FIELD

Magnetization dynamics is governed by the Landau-Lifshitz-Gilbert equation. Since magnetization  $\mathbf{M}$  is akin to angular momentum, we have an evolution equation for  $\mathbf{M}$  similar to angular momentum, the Bloch equation of motion  $d\mathbf{M}/dt = \gamma_0 \mathbf{M} \times \mathbf{H}$  with  $\gamma_0$  the gyromagnetic ratio and  $\mathbf{H}$  the external field (see for instance Kittel [4]).

Extending the Bloch equation to a moment  $\mathbf{M}$  subjected to an "effective" field  $\mathbf{H}_e$  and a dissipation term describing losses and relaxation processes in the material, Landau and Lifshitz (L-L) [5] assumed that dissipation is accounted for by a coefficient  $\lambda$  and introduced a dissipation non-linear term of the form  $\frac{\lambda\gamma_0}{\|\mathbf{M}\|} \mathbf{M} \times (\mathbf{M} \times \mathbf{H}_e)$  (where  $\|\mathbf{M}\|$  is the modulus of  $\mathbf{M}$ ) controlled by the effective magnetic field  $\mathbf{H}_e$ :

$$\frac{d\mathbf{M}}{dt} = -\gamma_0(\mathbf{M} \times \mathbf{H}_e) + \frac{\lambda\gamma_0}{\|\mathbf{M}\|} \mathbf{M} \times (\mathbf{M} \times \mathbf{H}_e) \quad (1)$$

L-L define, as in Quantum Field Theory, the effective field  $\mathbf{H}_e$  from the functional derivative of the total energy with respect to magnetization  $\mathbf{H}_e = -\delta E/\delta \mathbf{M}$ ; hence in any magnetic problem the total energy should be the starting point whether one is dealing with static or dynamical problems. In the simple Stoner particle case, the functional derivative reduces to the gradient with respect to  $\mathbf{M}$ ,  $\mathbf{H}_e = -\partial E/\partial \mathbf{M}$ .

In order to avoid the divergence problem arising in the L-L equation for the large dissipation case ( $\lambda \gg 1$ ), Gilbert modified the L-L dissipation term by introducing a damping term of the form  $\alpha\gamma \mathbf{M} \times (\frac{d\mathbf{M}}{dt})$ .

The equation of motion of a magnetic moment in presence of damping and effective field is given by the Landau-Lifshitz-Gilbert (L-L-G) equation:

$$\frac{d\mathbf{M}}{dt} = -\gamma(\mathbf{M} \times \mathbf{H}_e) + \alpha\gamma \mathbf{M} \times (\frac{d\mathbf{M}}{dt}) \quad (2)$$

where  $\mathbf{M}$  is the magnetization vector,  $\mathbf{H}_e$  the effective field,  $\gamma$  another gyromagnetic ratio and  $\alpha$  the damping parameter.

First of all, we retrieve Bloch equation in the simple case of zero damping and effective field  $\mathbf{H}_e = \mathbf{H}$  the externally applied field. In the static case, the L-L-G equation reduces to  $\mathbf{M} \times \mathbf{H}_e = 0$  meaning the static equilibrium condition is either  $\mathbf{M} // \mathbf{H}_e$  or  $\mathbf{H}_e = 0$  equivalent to the extremum (minimum) condition on the energy as discussed previously (see first part of this work).

The L-L-G equation conserves  $\|\mathbf{M}\| = \sqrt{\mathbf{M} \cdot \mathbf{M}}$  as seen by taking the scalar product on both terms of the RHS of

eq. 2. One gets  $\frac{d\mathbf{M}}{dt} \cdot \mathbf{M} = 0$  meaning that  $\|\mathbf{M}\| = M_s =$  constant, where  $M_s$  is the saturation magnetization.

The L-L-G equation seems odd from the mathematical point of view since one is used (in systems of ordinary differential equations or ODE) to see the first derivative term  $\frac{d\mathbf{M}}{dt}$  in the LHS only. Here it appears on both sides and pushes one to think that the system cannot be handled by standard mathematical integration tools like Euler or Runge-Kutta methods.

In addition, it is misleading to attempt at solving recursively the L-L-G equation by substituting repeatedly the term  $\frac{d\mathbf{M}}{dt}$  in the RHS of the equation. It is straightforward to show that the Landau-Lifshitz (L-L) equation is mathematically equivalent to the L-L-G equation by taking the cross product of the LHS of eq. 2 with  $\mathbf{M}$  and using  $\mathbf{M}$  norm conservation ( $\frac{d\mathbf{M}}{dt} \cdot \mathbf{M} = 0$ ). We obtain:

$$\mathbf{M} \times \frac{d\mathbf{M}}{dt} = -\gamma \mathbf{M} \times (\mathbf{M} \times \mathbf{H}_e) + \alpha\gamma M_s^2 (\frac{d\mathbf{M}}{dt}) \quad (3)$$

Substituting  $\mathbf{M} \times \frac{d\mathbf{M}}{dt}$  in eq. 2, we get:

$$\frac{d\mathbf{M}}{dt} = -\frac{\gamma}{1+\alpha^2} (\mathbf{M} \times \mathbf{H}_e) + \frac{\alpha\gamma}{1+\alpha^2} \mathbf{M} \times (\mathbf{M} \times \mathbf{H}_e) \quad (4)$$

It is now a matter of interpreting the coefficients appearing in the L-L or the L-L-G equations that will make them differ in a given situation. If one identifies  $\gamma_0$  as  $\frac{\gamma}{1+\alpha^2}$  and  $\lambda\gamma_0$  as  $\frac{\alpha\gamma}{1+\alpha^2}$  then both equations are same but if one insists on keeping  $\gamma_0$  as the gyromagnetic ratio or confusing dissipation ( $\lambda$ ) and damping ( $\alpha$ ) then the equations will differ since the factors affecting both terms in the RHS are numerically different.

In addition, the L-L dissipation term goes to zero when the damping coefficient goes to infinity making the L-L-G equation appear more physically appealing than the L-L equation.

The system of ODE eqs. 4 is integrable by standard explicit methods, such as Euler or Runge-Kutta (see for instance ref. [6]) after expressing the components in Cartesian coordinates. The conservation of the norm is very useful during integration (specially in explicit integration schemes) to test the accuracy and stability of integration.

$$\begin{pmatrix} \dot{m}_x \\ \dot{m}_y \\ \dot{m}_z \end{pmatrix} = -\frac{\gamma H_K}{(1+\alpha^2)} \times \begin{pmatrix} (1+\delta_x^2) & -(\delta_z - \delta_x \delta_y) & (\delta_x \delta_z + \delta_y) \\ (\delta_z + \delta_x \delta_y) & (1+\delta_y^2) & -(\delta_x - \delta_y \delta_z) \\ (\delta_x \delta_z - \delta_y) & (\delta_x + \delta_y \delta_z) & (1+\delta_z^2) \end{pmatrix} \times \begin{pmatrix} m_y h_{ez} - m_z h_{ey} \\ m_z h_{ex} - m_x h_{ez} \\ m_x h_{ey} - m_y h_{ex} \end{pmatrix} \quad (5)$$

with the definitions:  $\mathbf{m} = \mathbf{M}/M_s$ ,  $\dot{\mathbf{m}} = \frac{d\mathbf{m}}{dt}$ ,  $\mathbf{h}_e = \mathbf{H}_e/H_K$  and  $\delta_x = \alpha(M_x/M_s)$ ,  $\delta_y = \alpha(M_y/M_s)$ ,  $\delta_z = \alpha(M_z/M_s)$ .

Using order-4 Runge-Kutta (RK4) method (see ref. [6]) with  $\mathbf{M}$  along the  $z$ -axis as an initial condition, we apply at  $t = 0$  a time dependent field making  $135^\circ$  with the  $z$ -axis (see first part of this work). The 3D response of the magnetization in time is depicted in fig. 1 and the  $z$ -component of  $\mathbf{m}$  is depicted in fig. 2. Undesirable ringing effects (oscillations) in the time variation of  $\mathbf{m}$  are observed. They are so because they introduce an unwanted delay in magnetization reversal.

In order to eliminate the ringing effect, we move on to another reversal mode called precession switching in which the field is applied perpendicularly to the initial magnetization and whose action is on until the magnetization is reversed without displaying any ringing effect. The reversal path on the unit sphere is called a ballistic path (see fig. 3) emphasizing its optimality. The sensitivity of this process stems from the fact, the field must be switched off exactly at the time magnetization reverses (see fig.4).

### III. EFFECT OF TEMPERATURE ON MAGNETIZATION DYNAMICS

A grain at finite temperature is prone to thermal excitations that might alter its magnetization state. The simplest model describing the effect of temperature on a grain is inspired from Chemistry and is called the Néel-Arrhenius thermal excitation model.

At very low temperature, switching may occur by tunneling at a given energy through the energy barrier separating two magnetization states corresponding to two energy minima (see fig. 5). This is known as Macroscopic Quantum Tunneling of Magnetization that we will not describe here but for which there exist many reviews (see for instance ref. [2]).

At finite temperature, the empirical Arrhenius model is used to describe the kinetics of a thermally activated process. This assumes that an energy barrier hinders the forward progress of a chemical reaction. The height of this energy barrier is a measure of resistance to the reaction. Forward progress of the reaction requires the supply of an activation energy to surmount this barrier. It has the form [7]:

$$\tau = \tau_0 \exp(\Delta E/k_B T) \quad (6)$$

where  $\tau$  is the chemical reaction "inverse rate",  $\tau_0$  is the attempt time to traverse the barrier,  $\Delta E$  is the barrier height,  $k_B$  is Boltzmann constant and  $T$  is absolute temperature.

Drawing an analogy from radioactivity, one might view switching as a decay process with a typical probability of decay  $\lambda$ . Starting from an assembly of grains  $N_0$  at  $t = 0$ , the number of particles that decay in the instant  $[t, t + dt]$  is  $dN = -\lambda N(t)dt$ . Integrating with the initial condition  $N_0 = N(t = 0)$  we find that the particles that are still present (did not decay or switch)

is given by  $N(t) = N_0 \exp(-\lambda t)$ . This analogy holds if switching is treated as an irreversible process like decay. This means, switching back to the original value is not considered as a valid process. This is the case of data recording: If the stored value has changed once, it is no longer valid and must be rejected.

Since the average lifetime is given by  $\tau = 1/\lambda$  we interpret the inverse rate as the average lifetime with respect to switching. This means that the recorded information in a magnetic material (tape, hard disk, floppy etc...) stays unaltered for a period of time given by  $\tau$ . We infer from this analogy that the probability of switching is given by  $\exp(-t/\tau)$  and therefore the probability of retaining the information (not switching) is given by the complementary probability:  $P(t) = 1 - \exp(-t/\tau)$  with the new interpretation of Arrhenius formula  $\tau = \tau_0 \exp(\Delta E/k_B T)$ .

This decay picture of switching can be recast in a two-level model since switching means we have a transition from a magnetization state (1) to another (2) as depicted in fig. 5.

Considering a number (normalized) of non-interacting grains in state (1) as  $n_1$  and the number of grains in state (2) as  $n_2$  we may write a kinetic equation (Master equation) with typical transition times  $\tau_1, \tau_2$  as:

$$\frac{dn_1}{dt} = \frac{n_1}{\tau_1} - \frac{n_2}{\tau_2} \quad (7)$$

Assuming total number (normalized) conservation:  $n_1 + n_2 = 1$ , the solution of this equation is given by:

$$n_{1,2} = \frac{\tau_{1,2}}{\tau_1 + \tau_2} \pm [n_{1,0} - \frac{\tau_1}{\tau_1 + \tau_2}] \exp(-t/\tau) \quad (8)$$

where  $n_{1,0}$  is the initial value of  $n_1$  i.e.  $n_{1,0} = n_1(t = 0)$ . It is interesting to note that the decay time  $\tau = \frac{\tau_1 \tau_2}{\tau_1 + \tau_2}$  is the geometric average of  $\tau_1$  and  $\tau_2$ .

As a result, we obtain a simple classification of the possible magnetic states:

- We have a blocked state when  $\tau \gg t$  i.e.  $n_1 = n_{1,0} \forall t$ .
- We have a super-paramagnetic state in the opposite case  $\tau \ll t$  leading to  $n_{1,2} = \frac{\tau_{1,2}}{\tau_1 + \tau_2}$ .

Physically,  $t$  is of the order of the experimental measurement time and a blocked state means that no change to the system is observed during  $t$ . On the other hand, when the intrinsic time  $\tau \ll t$ , the magnetization change is so frequent that no well defined state is maintained for a long enough time. Thus the system behaves like a paramagnetic system that cannot store information (in a stable and reliable way). Hence the origin of the "super-paramagnetic" qualifier.

When a grain switches we have information storage errors and the bit error rate (BER) is given by the switching probability  $\exp(-t/\tau)$ .

In order to appreciate the meaning of BER and therefore average lifetime and barrier height, suppose we impose a BER of  $10^{-12}$ . This means one bit is wrong in a hard disk of 125 GBytes capacity. Identification of BER and switching probability  $\exp(-t/\tau)$  means that  $t = 10^{-12} \times \tau$ . According to eq. 6 and with the assumptions:  $\tau_0 \sim 10^{-9}$  sec and  $\Delta E/k_B T = 68$  we get  $t \sim \pi \times 10^8$  secs which means about 10 years of storage (1 year  $\sim \pi \times 10^7$  secs).

### A. Thermal average of the hysteresis loop

Thermal fluctuations induce random orientations of a Stoner particle. If the change of orientation is fast with respect to our appreciation of the hysteresis loop, then we observe an overall mean behaviour stemming from an average hysteresis loop. This average hysteresis loop can be calculated with several methods. In ensemble averaging, one considers a single grain in many orientational configurations that is making different angles with the magnetic field (taken along the z-direction). With time averaging, one considers a single grain undergoing different magnetization cycles while the magnetic field is making different angles with the grain axis. Under the Ergodic hypothesis (see ref. [8]) these averaging techniques should yield the same result. Adopting the ensemble average, we ought to find for each angle  $\phi$  the minimum energy angle  $\theta$  and every point on the hysteresis loop is made from the average over values of  $\phi$ . We perform the averaging in 3D following the original work of Stoner-Wohlfarth despite the fact our previous description was intentionally limited to 2D.

Taking the anisotropy axis along the grain long axis with polar angle  $\alpha$  and azimuthal angle  $\phi$  (see fig. 6) let  $p(\alpha, \phi)$  denote the PDF (probability density function) of the angles  $\alpha, \phi$  be uniform over the domains  $[0, \frac{\pi}{2}]$  (see note [11]) and  $[0, 2\pi]$ . Hence, the average loop (being the projection of the magnetization over the direction of the field) is given by:

$$\overline{\cos(\theta + \alpha)} = \frac{\int_0^{2\pi} d\phi \int_0^{\frac{\pi}{2}} \sin(\alpha) d\alpha \cos(\theta + \alpha) p(\alpha, \phi)}{\int_0^{2\pi} d\phi \int_0^{\frac{\pi}{2}} \sin(\alpha) d\alpha p(\alpha, \phi)} \quad (9)$$

Since the individual PDF are independent, the joint PDF:  $p(\alpha, \phi) = p_\alpha(\alpha)p_\phi(\phi)$  is decoupled and since both PDF are flat, we get:

$$\overline{\cos(\theta + \alpha)} = \int_0^{\pi/2} \cos(\theta + \alpha) \sin(\alpha) d\alpha \quad (10)$$

The algorithm is now clear: Sweeping over  $\alpha$  we find the angle  $\theta$  that minimises the energy in order to perform the integral. In order to optimize the number of arithmetic operations, we rather do the following. We transform the minimum equation (as done in the first part) in the form:  $\sin(\theta) \cos(\theta) + h \sin(\theta + \alpha) = 0$  through the replacement:

$m = \cos(\theta + \alpha)$  obtaining the equation:

$$h_{\uparrow, \downarrow} = -m \cos(2\alpha) \pm \frac{(2m^2 - 1)}{2\sqrt{1 - m^2}} \sin(2\alpha) \quad (11)$$

with the plus sign for the upper branch and the minus sign for the lower branch. Sweeping over values of  $m$  since  $|m| < 1$  allows us to find the corresponding values of  $h$  from which we keep only the minima energy values satisfying the equation:  $\cos(2\theta) + h \cos(\theta + \alpha) \geq 0$ . This gives us a table that with proper bookkeeping will help us find the average loop. The result of the averaging is displayed in the fig. 7 and compared in detail (see the figure caption) to the SW work.

### B. Langevin dynamics for the L-L-G equations

At finite temperature, the deterministic L-L-G equation is replaced by the stochastic Langevin equation [8] governing the evolution of  $\mathbf{M}$ . The effect of temperature is contained in a random additional field  $\boldsymbol{\eta}$  (stemming from thermal white noise) acting on  $\mathbf{M}$ :

$$\frac{d\mathbf{M}}{dt} = -\gamma_0(\mathbf{M} \times [\mathbf{H}_e + \boldsymbol{\eta}]) + \frac{\lambda\gamma_0}{\|\mathbf{M}\|} \mathbf{M} \times (\mathbf{M} \times \mathbf{H}_e) \quad (12)$$

where the additional magnetic field  $\boldsymbol{\eta} = (\eta_x, \eta_y, \eta_z)$  is defined by:

$$\langle \eta_i \rangle = 0, \quad \langle \eta_i(t) \eta_j(t') \rangle = 2\Delta \delta_{ij} \delta(t - t') \quad (13)$$

where  $\Delta$  is the white noise intensity given by [9]  $\Delta = \lambda k_B T / \gamma_0 M_s$  and  $(i, j = x, y, z)$ .

Let  $(\theta, \phi)$  be the spherical angles of the orientation of the moment  $\mathbf{M}$ . One may view  $(\theta, \phi)$  as a point on the surface of the unit sphere. A statistical ensemble of moments with different orientations can be represented by a distribution of points over the unit sphere  $W(\theta, \phi, t)$  at time  $t$ . Conservation of probability leads to a continuity equation:

$$\frac{\partial W}{\partial t} + \nabla \cdot \mathbf{J} = 0 \quad (14)$$

similar to electric charge continuity equation. The above is in fact a Fokker-Planck (F-P) partial differential equation (PDE) as shown below. The (probability) current density definition  $\mathbf{J} = W\mathbf{v}$  uses the velocity  $\mathbf{v} = \frac{1}{M_s} \frac{d\mathbf{M}}{dt}$  of the point  $(\theta, \phi)$  on the sphere, whereas  $W$  plays the role of a charge density.

Let us specialize to the case of a single angular degree of freedom and apply standard methods,[10] to write the PDE for the conditional probability density  $P \equiv P(x', t|x, 0)$ . The latter expresses the probability density of observing  $x' = \theta$  (at time  $t$ ) given the initial

state  $x = \psi$  (at time  $t = 0$ ). We get the following F-P equation:

$$\frac{\partial P}{\partial t} = A(x) \frac{\partial P}{\partial x} + \frac{1}{2} B(x) \frac{\partial^2 P}{\partial x^2} \quad (15)$$

The "mean first passage time" (time, for the Stoner particle, to switch)  $T(x)$  satisfies an ODE given by (see ref. [10]):

$$A(x) \frac{dT(x)}{dx} + \frac{1}{2} B(x) \frac{d^2 T(x)}{dx^2} = -1 \quad (16)$$

In our case,  $x = \psi$ ,  $A(\psi) = \frac{\lambda \gamma_0}{M_s} \frac{dE(\psi)}{d\psi} - \frac{\gamma_0^2 \Delta}{\tan(\psi)}$  where  $E(\psi)$  is the energy (per unit volume) of the Stoner particle,  $E(\psi) = -M_s H \cos(\psi) + K_{eff} \sin^2(\psi)$ , containing Zeeman and effective anisotropy terms.  $H$  is the externally applied field. Besides  $\frac{1}{2} B(\psi) = -\gamma_0^2 \Delta$  yield the equation for the "mean first passage time" as:

$$-\left[ \frac{\lambda \gamma_0}{M_s} \frac{dE(\psi)}{d\psi} - \frac{\gamma_0^2 \Delta}{\tan(\psi)} \right] \frac{dT(\psi)}{d\psi} + \gamma_0^2 \Delta \frac{d^2 T(\psi)}{d\psi^2} = +1 \quad (17)$$

This second order ODE can be transformed into a first-order equation in  $v(\psi) = dT/d\psi$  and integrated once with the initial condition  $v(\psi = 0) = 0$ :

$$v(x) = \frac{1}{\sin(x)} \left[ \exp(-f(x)) \int_x^0 \frac{\sin y}{\gamma_0^2 \Delta} \exp(f(y)) dy \right] \quad (18)$$

with:

$$f(x) = \frac{\lambda}{4\gamma_0 V \Delta} (4HV \cos x + \beta M_s \cos 2x + \beta M_s) \quad (19)$$

$V$  is the volume of the particle and  $\beta = \frac{2V K_{eff}}{M_s^2}$ .

Integrating once again to get  $T(x)$  and using the definition of the thermal transit time  $t_{th}$  as the value  $T(x = 0)$ , we obtain:

$$t_{th}/c = a \int_{\cos(\theta_0)}^1 dx \frac{e^{-a(x+b)^2}}{(1-x^2)} \int_x^1 dy e^{a(y+b)^2} \quad (20)$$

The angle  $\theta_0$  maximizes the stationary PDF  $\exp[-E(\theta)/k_B T] \sin(\theta)$  and is also given by the condition  $T(\theta_0) = 0$ . The coefficients  $a, b, c$  are given respectively by:

$$a = \frac{K_{eff}}{k_B T}, b = \frac{H M_s}{2K_{eff}}, c = \frac{M_s}{\gamma_0 \lambda K_{eff}} \quad (21)$$

It is interesting to analyze the results at high and low temperatures. In the high temperature limit ( $a \sim 0$ ); we get:  $t_{th} \sim ca \ln(2)$ ; whereas at low temperature ( $a(1+b)^2 \gg 1$ ), we obtain:

$$t_{th} = \frac{c}{2} \sqrt{\frac{\pi}{a}} \frac{1}{(1-b^2)} \frac{1}{(1+b)} \exp[a(1+b)^2] \quad (22)$$

Identifying the thermal transit time with  $\tau$  we recover in that way the Néel-Arrhenius expression:

$$t_{th} \sim \tau = \tau_0 \exp(\Delta E/k_B T), \text{ where the prefactor} \\ \tau_0 = \frac{c}{2} \sqrt{\frac{\pi}{a}} \frac{1}{(1-b^2)} \frac{1}{(1+b)}, \quad (23)$$

and the barrier height  $\Delta E = K_{eff}(1+b)^2$  at low temperatures.

In the case of arbitrary temperature, the behaviour of the transit time versus  $a$  (inverse temperature) for various field-anisotropy ratios  $b$  is obtained numerically as depicted in fig. 8.

One might be tempted to define the thermal switching time directly from the behaviour of the probability versus time since the F-P equation provide a means to obtain that behaviour. Switching is reached when the probability  $P(\pi/2, t_s) = 0.5$ .

In fig. 9, the time dependence of the probability  $P(\pi/2, t)$  is displayed for the field-anisotropy ratio  $b = -0.4$  (see ref. [12]) and shows a very quick variation above some threshold time if one starts initially from all zero values of the probability.

The results are validated by comparison with the analytical case in fig. 10. Even if the steepness of the numerical results appear to be weaker than the analytical results, the graph provides a strong support for the approximate equivalence of both descriptions.

Analysis of the thermal switching time versus temperature has numerous technological consequences. Once again, the F-P equation provides this kind of information paving the way to the search of the best materials/conditions that yield the optimal switching time.

We perform direct time integration of the F-P equations to extract the behaviour of the switching time versus temperature. As an illustration, using the same field-anisotropy ratio  $b = -0.4$  as previously, the inverse switching time versus temperature is displayed in fig. 11.

#### IV. EXTENSIONS AND PERSPECTIVES OF THE STONER-WOHLFARTH MODEL

The SW model is a macrospin description of magnetic systems that is extremely rich from the static, dynamic and statistical viewpoints. Despite its numerous limitations (and of the macrospin approach in general) described in the first part of this work, it remains a valid starting point for the useful description and basic understanding of many (static and dynamic) problems of fundamental and applied magnetism.

The full 3D counterpart of the SW model as done in ref. [13] is an important extension and of great interest.

We point anew to the fact the averaging of the hysteresis loop done in section 3 related to thermal effects was performed in 3D as in SW work for comparison.

The extension to uniaxial anisotropies of arbitrary order (a higher anisotropy is of fourth or sixth order like in Cobalt ...) or other forms like biaxial, planar, cubic (as in solid Ni or Fe) or of several competing types might provide a richer behaviour of the loop versus angle.

The use of arbitrary non-ellipsoidal shape for the grain is also challenging given the occurrence of non-uniformity of the magnetization.

The interaction between grains must also be studied and gauged with respect to its role in affecting the switching of the magnetization. New types of interactions or novel types of exchange between grains or with other objects might be exploited in spintronic and quantum devices.

#### Acknowledgement

The authors wish to acknowledge W. D. Doyle (MINT, Alabama) for sending many papers of his work on fast switching and helpful correspondance.

- 
- [1] I. Zutic, J. Fabian and S. Das Sarma : Rev. Mod. Phys. Vol. **76**, 323 (2004).
- [2] E.M. Chudnovsky and L. Gunther: Phys. Rev. Lett. **60**, 661 (1988).
- [3] E. C. Stoner, and E. P. Wohlfarth, Phil. Trans. Roy. Soc. London **A240**, 599 (1948), reprinted in IEEE Trans. Magn. **27**, 3475 (1991).
- [4] C. Kittel, Introduction to Solid State Physics Wiley, New-York, p.404 (1996).
- [5] L. D. Landau and E. M. Lifshitz, Electrodynamics of Continuous Media, Pergamon, Oxford, p.157 (1975).
- [6] Numerical Recipes in C: The Art of Scientific Computing, W. H. Press, W. T. Vetterling, S. A. Teukolsky and B. P. Flannery, Second Edition, page 389, Cambridge University Press (New-York, 1992).
- [7] E. U. Condon, Am. J. Phys. **22**, 132 (1954).
- [8] F. Reif, Statistical and Thermal Physics (McGraw-Hill, New-York, 1985).
- [9] W.F. Brown Jr., Phys. Rev. **130**, 1677 (1963). Brown derived the thermal noise intensity expression by comparing the equilibrium distribution  $W$  to a Boltzmann's.
- [10] C. W. Gardiner, *Handbook of Stochastic Methods*, 2nd ed. (Springer-Verlag, Berlin, 1990).
- [11] The polar angle  $\alpha$  varies in general over the interval  $[0, \pi]$ . From symmetry it is restricted here to the interval  $[0, \frac{\pi}{2}]$ .
- [12] S. I Denisov and A.N. Yunda: Physica **B 245**, 282 (1998).
- [13] W. Wernsdorfer: Advances in Chemical Physics "Classical and quantum magnetization reversal studied in nanometer sized particles and clusters" Edited by Stuart A. Rice (Wiley Interscience, New-York 2001).

#### FIGURES

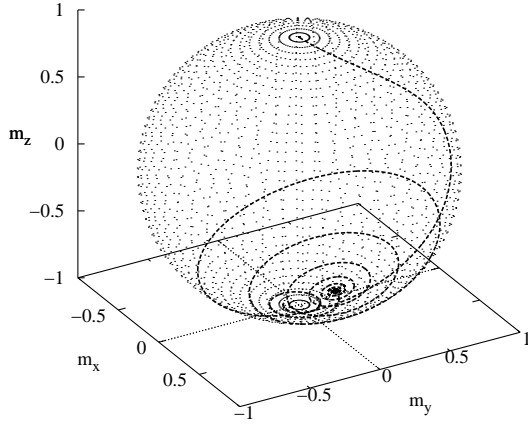


FIG. 1: Trajectory of the magnetization tip on the unit sphere for a field applied at  $t=0$  in the  $y$ - $z$  plane and making an angle of  $135^\circ$  with the  $z$ -axis. The damping is  $\alpha = 0.1$ , the field is in the  $yOz$  plane making an angle of  $135^\circ$  with  $z$ -axis. It is applied at  $t = 0$  for 9 nanosecs. Its value is  $0.5 H_K$ .

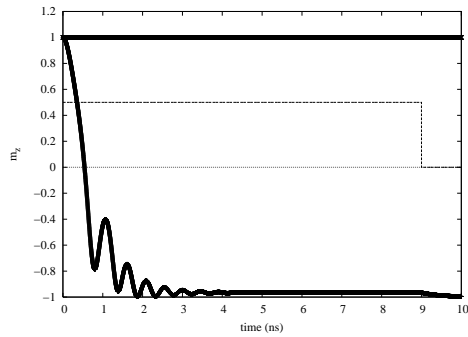


FIG. 2: Variation of the magnetization component  $m_z$  as a function of time. The parameters are the same as in fig. 1. The straight thick line indicates conservation of  $\|\mathbf{M}\|$  during integration. The dotted line is the variation of the applied magnetic field with time. The ringing observed due to damping is a major cause of delay in reversal.

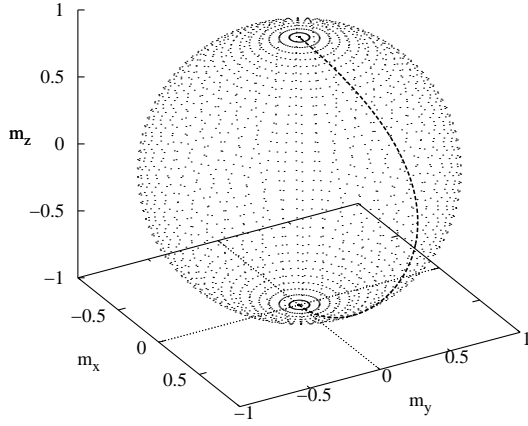


FIG. 3: Ballistic trajectory of the magnetization tip on the unit sphere for a field applied at  $t=0$  in the  $y$ - $z$  plane and making an angle of  $90^\circ$  with the  $z$ -axis. The damping is small:  $\alpha = 0.001$ , the field is in the  $yOz$  plane making an angle of  $90^\circ$  with  $z$ -axis. It is applied at  $t = 0$  for 0.12 nanosecs. Its value is  $1.7 H_K$ .

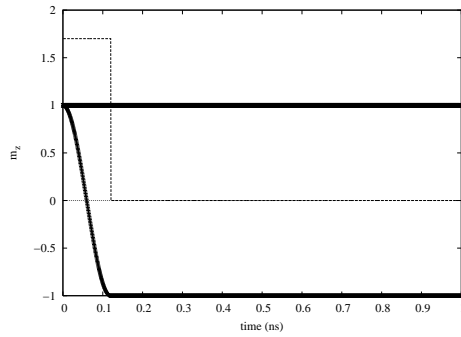


FIG. 4: Variation of the magnetization component  $m_z$  as a function of time. The parameters are the same as in fig. 3. The straight thick line indicates conservation of  $\|\mathbf{M}\|$  during integration. The dotted line is the variation of the applied magnetic field with time. No delay in magnetization reversal is observed due to the small damping suppressing the ringing.



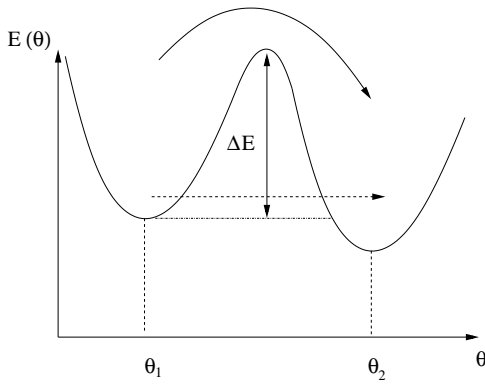


FIG. 5: Energy versus angle  $\theta$  showing the barrier  $\Delta E$  the system has to overcome in order to go from state (1) with  $\theta_1$  to state (2) with  $\theta_2$ . At low temperature the system can tunnel from state (1) to state (2).

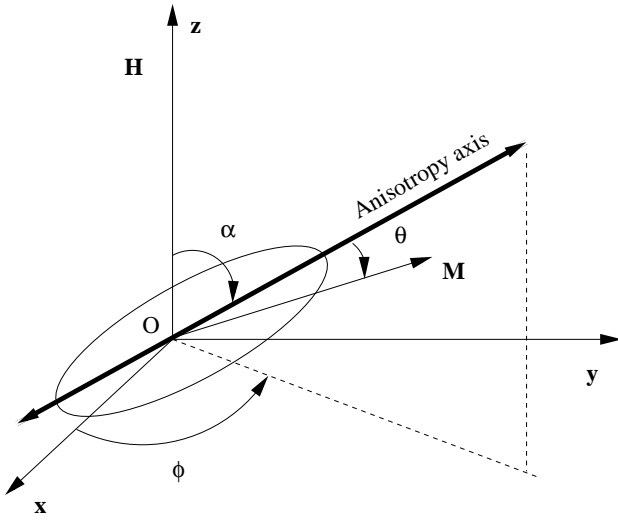


FIG. 6: System of coordinates displaying the anisotropy axis in 3D with the applied magnetic field  $\mathbf{H}$  along the  $z$ -axis and the magnetization  $\mathbf{M}$  all in the same vertical plane indicated by dashed lines and making the angle  $\phi$  with the  $xOz$  plane.

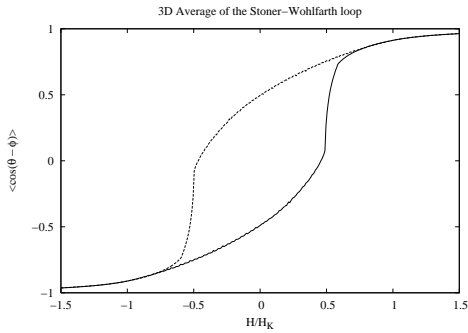


FIG. 7: The 3D averaged hysteresis loop looks very much like the Stoner-Wohlfarth curve except it is less rounded at the approximate switching field values.

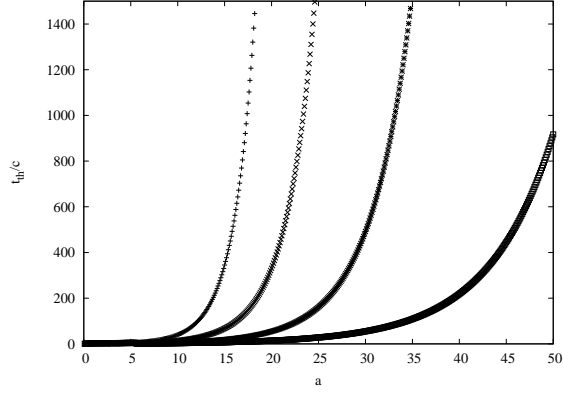


FIG. 8: Normalized thermal switching time  $t_{th}/c$  versus inverse temperature  $a$  for various field-anisotropy ratios  $b = -0.3, -0.4, -0.5, -0.6$  as we proceed from left to right.

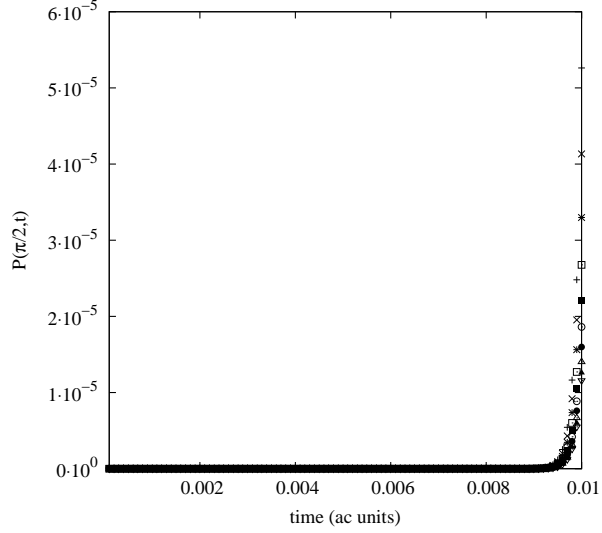


FIG. 9: Switching probability at  $\theta = \pi/2$  versus time at a fixed temperature for a field-anisotropy ratio  $b = -0.4$  (see ref. [12]). The ten curves corresponding to ten different inverse temperatures uniformly distributed over the interval  $a = [0 - 50]$  (see fig. 8) are indistinguishable. Switching time is reached when the probability is equal to  $1/2$ .

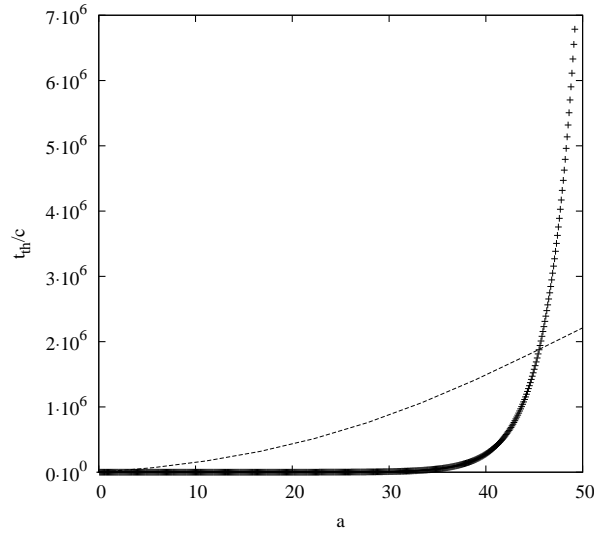


FIG. 10: Comparison between the analytical formula for the normalized thermal switching time  $t_{th}/c$  and the numerical integration of the F-P equation versus inverse temperature  $a$ . The analytical formula leads to a very steep variation with  $a$  in sharp contrast with the numerical case.

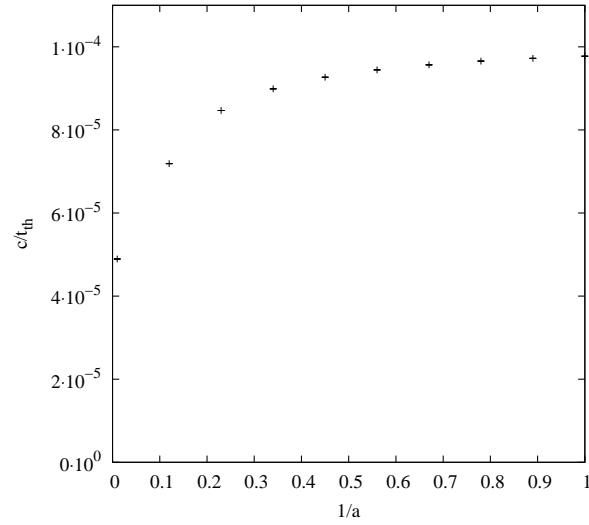


FIG. 11: Inverse normalized thermal switching time  $c/t_{th}$  versus temperature  $1/a$  for a field-anisotropy ratio  $b = -0.4$ .